DEVELOPMENT OF A TSUNAMI FORECAST MODEL FOR CRAIG, ALASKA

Chris Chamberlin

September 4, 2009

DRAFT

DRAFT

Contents

Abstract 5
1 Background and Objectives 5
2 Forecast Methodology 5
2.1 Historical tsunami records 6
2.2 Digital elevation models 6
2.2.1 Source digital elevation models 6
2.2.2 Reference model (RIM) grid 7
2.2.3 Forecast model (SIM) grid 7
2.3 Model Setup 10
3 Results 10
3.1 Model validation 10
3.2 Model stability and reliability 11
4 Summary and Conclusions 13
5 Acknowledgments 13
6 References 13
7 7.0 Appendix A 14

DRAFT

List of Tables

Table 1. Candidate forecast grids. Bathy nodes is the number of "wet" model grid nodes, excluding any runup. Max dt is the maximum model timestep allowed by this grid to remain within CFL condition. 8
Table 2. Comparison of candidate forecast (SIM) grid combinations with reference (RIM) grid combinations. Results for normalized timeseries RMS error and maximum wave error are divided into quartiles; above-average results are highlighted in gray. Model runtime (for four hours of model time) much be under ten minutes. Italicized grid combination, A1 B1 C1, is selected for use as the forecast model. 9
Table 3. MOST model setup summary 10
Table 4. Historical tsunami events modeled. Events for which tide gauge records are available at Craig are marked with *. 11
Table 5. Source combinations and maximum forecast wave heights (at Craig tide gauge) for stability and reliability test scenarios. See Gica *et al*. 2008 for details of source locations. Sources highlighted in bold were used for the grid sensitivity comparison described in section 2.2.3. 13

DRAFT

List of Figures

Figure 1. Location of Craig, Alaska, relative to other planned and completed forecast models. ... 16
Figure 2. (a) Location of Craig, Alaska on the west side of Prince of Wales Island, partially protected from the open ocean by several offshore islands. (b) Aerial photograph of Craig, showing the town center and location of the tide station operated by the West Coast/Alaska Tsunami Warning Center. ... 16
Figure 3. Comparison of bathymetry along southeastern Baranof Island. Original ETOPO1 bathymetry (dashed contours) is substantially improved in the model grid (solid contours) by the addition of existing medium-resolution bathymetry, and digitized points from NOS charts. ... 17
Figure 4. Reference inundation model (RIM) grid extents. ... 18
Figure 5. Extents of candidate forecast model (SIM) grids. Crosshatched area in (c) is the region where maximum wave comparisons with the reference model (RIM) are performed. See Table 1 for details of grid extents and resolutions. ... 19
Figure 6. Forecast model (SIM) grid extents. ... 2
Figure 7. Maximum wave heights at Craig tide gauge for M_w 8.3 seismic scenarios. ... 3
Figure 8. Maximum wave heights at Craig tide gauge for M_w 9.3 seismic scenarios. ... 3
Figure 9. 15 January 2009 Kuril tsunami. (a) Forecast model (SIM) maximum amplitude plot. (b) Reference model (RIM) maximum amplitude plot. (c) Wave amplitude at tide gauge. Green: Forecast model (SIM); Red: Reference model (RIM); Black: tide gauge record. ... 4
Figure 10. 15 August 2007 Peru tsunami. (a) Forecast model (SIM) maximum amplitude plot. (b) Reference model (RIM) maximum amplitude plot. (c) Wave amplitude at tide gauge. Green: Forecast model (SIM); Red: Reference model (RIM); Black: tide gauge record. ... 5
Figure 11. 1 April 2007 Solomon tsunami. (a) Forecast model (SIM) maximum amplitude plot. (b) Reference model (RIM) maximum amplitude plot. (c) Wave amplitude at tide gauge. Green: Forecast model (SIM); Red: Reference model (RIM). ... 5
Figure 12. 15 November 2006 Kuril tsunami. (a) Forecast model (SIM) maximum amplitude plot. (b) Reference model (RIM) maximum amplitude plot. (c) Wave amplitude at tide gauge. Green: Forecast model (SIM); Red: Reference model (RIM). ... 6
Figure 13. 3 May 2006 Tonga tsunami. (a) Forecast model (SIM) maximum amplitude plot. (b) Reference model (RIM) maximum amplitude plot. (c) Wave amplitude at tide gauge. Green: Forecast model (SIM); Red: Reference model (RIM). ... 6
Figure 14. 17 November 2003 Rat Island tsunami. (a) Forecast model (SIM) maximum amplitude plot. (b) Reference model (RIM) maximum amplitude plot. (c) Wave amplitude at tide gauge. Green: Forecast model (SIM); Red: Reference model (RIM). ... 7
Figure 15. 10 June 1996 Andreanof tsunami. (a) Forecast model (SIM) maximum amplitude plot. (b) Reference model (RIM) maximum amplitude plot. (c) Wave amplitude at tide gauge. Green: Forecast model (SIM); Red: Reference model (RIM). ... 7
Figure 16. 4 October 1994 Kuril tsunami. (a) Forecast model (SIM) maximum amplitude plot. (b) Reference model (RIM) maximum amplitude plot. (c) Wave amplitude at tide gauge. Green: Forecast model (SIM); Red: Reference model (RIM). ... 8
Figure 17. 28 March 1964 Alaska tsunami. (a) Forecast model (SIM) maximum amplitude plot. (b) Reference model (RIM) maximum amplitude plot. (c) Wave amplitude at tide gauge. Green: Forecast model (SIM); Red: Reference model (RIM). ... 8
Figure 18. 1 April 1946 Unimak tsunami. (a) Forecast model (SIM) maximum amplitude plot. (b) Reference model (RIM) maximum amplitude plot. (c) Wave amplitude at tide gauge. Green: Forecast model (SIM); Red: Reference model (RIM). ... 9

DRAFT

Development of a Tsunami Forecast Model for Craig, Alaska

Chris Chamberlin

DRAFT

Abstract

This report describes the development and validation of a tsunami inundation forecast model (also called a Stand-By Inundation Model; SIM) for the town of Craig, Alaska. The resulting inundation model will be used as part of the Short-term Inundation Forecasting for Tsunamis (SIFT) system being developed for NOAA's tsunami warning centers. The development process includes compilation of bathymetric and topographic data and creation of higher-resolution reference model (RIM) grids, and lower-resolution forecast model (SIM) grids capable of producing an inundation forecast in minutes. The study included the development of metrics for comparing the results of various forecast grid configurations to determine the best forecast grid setup. Model testing compared the forecast results to reference results for several historical tsunamis, and tested the forecast model for numerical stability for a range of possible moderate and large tsunamis.

1 Background and Objectives

The objective of this study is to develop a tsunami forecast model for Craig, Alaska, capable of producing accurate tsunami wave height, current, and inundation forecasts in real time. The forecast model will be used as part of the Short-term Inundation Forecasting for Tsunamis (SIFT) system currently being developed by NCTR for NOAA's tsunami warning centers. Synolakis *et al* (2007) and Tang *et al* (2009) provide details of NOAA's tsunami forecast methodology.

Craig is located on the west coast of Prince of Wales Island, in southeast Alaska. Located approximately 100 km north of Dixon Entrance, which forms the United States-Canada border, it is the southernmost forecast model location currently planned for Alaska (Figure 1). Nearby forecast models include a proposed model at Port Alexander, 125 km northwest, and a completed model at Sitka, 220 km northwest (Burwell 2008).

At the 2000 census, Craig had a population of 1,397 people, making it the largest population center on Prince of Wales Island. The town center is built on a small peninsula with a maximum elevation of approximately 18 m above mean high water. The town has two small-boat harbors, Shelter Cove on the south side of the peninsula, and North Cove on the north side. Shelter Cove is protected by two stone breakwaters; North Cove's floating breakwater was formerly part of the I-90 floating bridge across Lake Washington, near Seattle (AP 2002). Transportation facilities include seaplane service to Ketchikan and a road connection to the ferry terminal on the east side of Prince of Wales Island.

There is a tide gauge, operated by the West Coast/Alaska Tsunami Warning Center, located at Craig (see section 2.1).

The town is located on the northeast side of Bucareli Bay, approximately 40 km from the bay's opening into the Pacific Ocean; it is partially protected from the open ocean by several offshore islands (Figure 2). The bay has a minimum width of 3 km between Craig and the ocean, and the bay is deep (at least 100 m deep) throughout much of its area. There are also several narrower, shallower waterways connecting the town to the Pacific Ocean.

2 Forecast Methodology

The tsunami forecast model used in SIFT runs on the MOST numerical model. In the version of MOST currently in use in SIFT, a tsunami model consists of three nested grids describing the bathymetry and topography of the area. The

DRAFT

outermost grid, designated the A grid, has the largest extent and lowest resolution; the B grid is an intermediate grid, and the C grid the highest resolution. Input boundary conditions for the A grid are computed by linear combination and scaling of the results of one or more pre-computed ocean-wide wave propagation model runs (Gica *et al*. 2008).

Two complete sets of grids are created. First, a reference model is developed, using large extent and high resolution grids; this model, which takes several hours to run, is used as a baseline for creating a less computationally-intensive forecast model that can be used to produce real-time wave height forecasts. Comparison with the reference model, as well as historical tide gauge records where available, provide assurance that reducing the forecast model grid resolution and extent does not substantially change the overall forecast.

2.1 Historical tsunami records

Compared to many other forecast model sites in Alaska, Craig has a limited historical tsunami record. This is primarily due to the lack of a tide gauge installation near the town until 2006.

According to media reports at the time, the 1964 Alaska tsunami produced a fourteen-foot (4.3 m) wave on the southeast side of the Craig town center, inundating the coastal road (Lander 1996). No other records of this major tsunami's impact at Craig are available.

In March 2006 the West Coast/Alaska Tsunami Warning Center (WCATWC) installed a tide gauge on a City of Craig-owned dock 1.5 km north of the town center, at 55.4888° N, 133.1423° W (Paul Whitmore, pers. comm.). This gauge uses a downward-looking radar sensor to deliver real-time water height readings at 15 s intervals. The National Ocean Service (NOS) operated a tide station nearby for two months in 2007 for the purpose of establishing tidal datums and harmonic constituents, but NOS does not operate a primary tide station at Craig. The nearest primary NOS stations are at Ketchikan and Port Alexander.

Water level records for three tsunami events were provided to NCTR by WCATWC (Table 4). These three recent events, all of which had sources far from Craig, produced no substantial waves at Craig; in all three cases, it is difficult to discern a tsunami signal in the instrument noise. Although they occurred after the installation of the Craig tide gauge, records for the 2006 Kuril and 2007 Kuril events are not available due to hardware failure.

The tidal component of the timeseries records was removed using a high-pass Butterworth filter to remove wavelengths longer than 1 to 2 hours, depending on the input timeseries.

2.2 Digital elevation models

The MOST numerical tsunami model used for forecasting uses a series of three nested bathymetric/topographic digital elevation model grids. These grids are derived from several sources.

2.2.1 Source digital elevation models

Forecast model grids were derived from several source digital elevation models (DEMs). The National Geophysical Data Center (NGDC) provided two DEMs covering Craig; one with a smaller extent at a resolution of 1/3 arc-second, and one with a larger extent at a resolution of 1 arc-second (Taylor et al. 2008). These DEMs, designed specifically for tsunami inundation modeling, were derived from multiple sources, primarily NOS bathymetric surveys and Shuttle

DRAFT

Radar Topography Mission (SRTM) topography. Depths in the grids developed by NGDC are relative to local mean high water (MHW); resulting wave height forecasts are also relative to this datum.

A lower-resolution grid with a large extent, suitable for the outermost model grid, was derived from several sources. The base grid was developed by resampling the ETOPO1 global 1-minute dataset (Amante and Eakins, 2008). In the ocean off southeast Alaska, ETOPO1 bathymetry is primarily estimated from satellite altimetry readings (Smith and Sandwell, 1997).

The ETOPO1 dataset provides broad bathymetry coverage, but exhibits substantial smoothing near the coast in regions with steep nearshore topography. To improve modeling of wave dynamics on the outer coast adjacent to Craig, additional datasets were included. An existing 9 arc-second DEM for the Sitka Sound (central Baranof Island) area, developed by PMEL in 2005, was resampled and overlaid on the ETOPO1 dataset. Charted soundings and contours from NOS charts #17320 and #501 were used to correct nearshore bathymetry along the southwest coast of Baranof Island, and the northwest coast of the Queen Charlotte Islands. These corrections corrected the location of the 50 meter contour up to 10 km closer to shore (Figure 3).

2.2.2 Reference model (RIM) grid

From the source grids described in section 2.3, a set of three nested high-resolution model grids were created (Figure 4). These reference grids provide guidance for the development of optimized forecast grids of lower resolution and smaller extent that will allow the model to operate in real time (Tang *et al*. 2009). Table 2 shows the model grids and setup parameters for the reference model.

Reference model run time to model 4 hours of tsunami propagation is approximately 14 hours on a 2.9GHz Intel Xeon processor.

2.2.3 Forecast model (SIM) grid

The forecast model is required to produce wave height and inundation forecasts similar to the reference model, for 4 hours of model time, in less than 10 minutes of computation time. To achieve this requirement, the forecast model grids are of lower resolution and a more limited extent than the reference model.

To determine the forecast grid extents and resolutions that will best reproduce the results from the higher-resolution reference model, several candidate forecast grids were created (Figure 5). These candidate forecast grids were designed to capture a several potential techniques for achieving the computational performance requirements, including some grids with larger extents and lower resolution, and others with smaller extent and higher resolution (Table 1). In all, eight candidate grids were created; three A grids, two B grids, and three C grids.

To evaluate the accuracy with which each candidate forecast model reproduces the results of the reference model (Section 2.2.2), each combination of A, B, and C grids (18 combinations) was tested with six event scenarios, resulting to in a total of 108 test runs. The six test scenarios, highlighted in Table 5, are intended to capture a range of source locations and magnitudes.

In the operational SIFT system, inundation models produce two major products: a maximum-amplitude plot including inundation extents, and a timeseries at the warning point (tide gauge) location, showing wave arrival times and heights. To

DRAFT

compare the forecasted results of the various grid combinations with the reference model, two metrics reflect these two major products; a third covers the forecast speed requirements.

Normalized RMS error: This is the root-mean-square error of the forecasted timeseries at the Craig tide gauge location, compared to the reference model. Because the wave heights vary substantially between the scenarios, the RMS error is normalized by the overall wave amplitude. The RMS error is calculated for four hours of modeled time.

Maximum wave error: The percentage error in maximum wave forecast, compared to the reference model, is calculated for the area of greatest interest around the town of Craig. This area of interest is highlighted by crosshatching in Figure 5c.

Run time: This is the time, in minutes, required for the forecast model to produce four hours of wave dynamics; under the model design goals used for previous inundation models in the SIFT system, the forecast model should generate four hours of modeled time in ten minutes of compute time. The model was tested on a 2.93 GHz Intel Xeon processor, similar to that currently installed at the Tsunami Warning Centers.

Table 2 shows the results of the forecast model comparisons. Average RMS and maximum wave errors are computed over the six scenarios, for each grid combination. Maximum errors highlight the result of the poorest forecast among the scenarios; this is intended to eliminate those grid combinations that perform very poorly for some source scenarios. The results are highlighted by quartile (25th, 50th, 75th percentile), where the first quartile is the best result. Run times under the ten minute requirement are highlighted.

The results show three grid combinations that rank in the top quartile for each metric; all of them use grids B1 and C1; the selection of the A grid has a lesser effect on the result. Grid combination A1 B1 C1 results in the lowest error values, and has a run time less than ten minutes, so we select that grid combination for the forecast model (Figure 6).

DRAFT

Grid	Extent	Cell size	Bathy nodes	Max dt (s)
A1	(223.02,57.65) - (227.88, 52.42)	2 min	17127	12.02
A2	(223.01, 57.20) - (227.89, 53.10)	1.5 min	23869	9.02
A3	(223.51, 57.20) - (227.61, 53.10)	1.5 min	20314	9.02
B1	(226.10, 55.72) - (227.05, 54.95)	12 sec	41977	3.51
B2	(225.90, 55.80) - (227.15, 54.70)	18 sec	38523	5.26
C1	(226.75, 55.56) - (226.91, 55.37)	3 sec	32481	1.14
C2	(226.78, 55.56) - (226.89, 55.39)	2 sec	48476	0.76
C3	(226.80, 55.57) - (226.91, 55.42)	2 sec	35411	0.88

Table 1. Candidate forecast grids. *Bathy nodes* is the number of "wet" model grid nodes, excluding any runup. *Max dt* is the maximum model timestep allowed by this grid to remain within CFL condition.

Grid combination	Normalized RMS error avg	Normalized RMS error max	Max wave error avg	Max wave error max	Runtime (min)
A1 B1 C1	*2.01*	*6.45*	*0.19*	*0.37*	*8.5*
A1 B1 C2	4.58	10.87	0.24	0.40	14.7
A1 B1 C3	5.35	13.15	0.26	0.45	10.5
A1 B2 C1	2.79	10.15	0.29	0.51	7.0
A1 B2 C2	6.10	15.20	0.32	0.55	12.7
A1 B2 C3	6.13	15.97	0.31	0.59	9.3
A2 B1 C1	2.46	9.50	0.21	0.34	8.4
A2 B1 C2	6.16	13.65	0.28	0.42	13.9
A2 B1 C3	7.20	16.44	0.29	0.46	10.6
A2 B2 C1	3.05	12.11	0.27	0.41	7.0
A2 B2 C2	7.38	16.21	0.31	0.46	12.7
A2 B2 C3	8.95	27.29	0.29	0.48	9.8
A3 B1 C1	2.46	9.77	0.22	0.35	7.6
A3 B1 C2	5.93	13.07	0.28	0.41	14.4
A3 B1 C3	6.87	14.83	0.30	0.46	9.5
A3 B2 C1	3.06	12.81	0.28	0.47	7.4
A3 B2 C2	6.81	14.34	0.32	0.52	12.8
A3 B2 C3	8.53	25.51	0.30	0.53	9.5
	Error quartiles:				Runtime:
	1st (best)	2nd	3rd	4th (worst)	< 10 min
					> 10 min

Table 2. Comparison of candidate forecast (SIM) grid combinations with reference (RIM) grid combinations. Results for normalized timeseries RMS error and maximum wave error are divided into quartiles; above-average results are highlighted in gray. Model runtime (for four hours of model time) much be under ten minutes. Italicized grid combination, A1 B1 C1, is selected for use as the forecast model.

DRAFT

2.3 Model Setup

Table 3 summarizes the grid extents and model parameters of the reference and forecast models. The model parameters are similar to those used for other models in the SIFT system. A slightly higher Manning (friction) coefficient is used in the reference model to reduce high-frequency, small-amplitude ringing that occurs along shorelines in the reference C grid with a lower coefficient.

	Reference Model (RIM)			**Forecast Model (SIM)**		
Grid	Coverage Long. (W) Lat. (N)	Cell size	Time step (s)	Coverage Long (W) Lat (N)	Cell size	Time step (s)
A	137W-132.1W 52.4N - 57.7N	24 s	2.25	137W-132.1W 52.4N - 57.7N	120 s	6.0
B	134.1W-132.9W 54.7N - 55.8N	3s	0.75	133.9W-133.0W 52.4N - 57.6N	12 s	3.0
C	133.3W-132.0W 55.4N - 55.6N	1s	0.25	133.25W-133.1W 55.36N - 55.55N	3 s	1.0
Minimum offshore depth (m)	2.0			2.0		
Water depth for dry land (m)	0.1			0.1		
Manning coefficient (*n)*	0.002			0.0015		
CPU time for 4 hour simulation	14 hours			8.5 minutes		

Table 3. MOST model setup summary

DRAFT

3 Results

Validation of the forecast model ensures that, to the greatest extent possible, the model accurately reproduces actual tsunami events, and that it remains numerically stable under all possible source conditions (Synolakis *et al* 2007; Tang *et al* 2009).

3.1 Model validation

To validate the forecast model, comparisons with reference model runs of ten historical tsunamis were performed (Table 4). Figures 9 – 18 show the maximum wave values computed for each event by the forecast and reference models, and the wave height timeseries computed at the current tide gauge location.

As described in section 2.1, tide gauge records were available for three events: 15 January 2009 Kuril, 15 August 2007 Peru, and 3 May 2006 Tonga. Figures 9, 10, and 13 show reference and forecast model runs of these events along with the tide gauge timeseries provided by WCATWC.

For all three events, the forecast tsunami wave height is smaller than the approximately 3 cm noise evident in the signal after detiding; thus, these

signals are of limited value for model validation. The 2006 Tonga record shows a peak and trough arriving at 13 hours and 14 hours, respectively, which match the modelled first wave arrival times.

Event	Time (UTC)	Mw	Lon.	Lat.	Source
Kuril *	2009/01/15 17:49:39	7.5	155.156E	46.862N	kiszb12*0.92 + kiszb13*0.19
Peru *	2007/08/15 23:40:57	8.1	76.509W	13.354S	cssza62*4.3 + csszb62 * 4.1
Solomon	2007/04/01 20:40:41	8.2	156.4E	7.96S	nvszb10 * 12.0
Kuril	2006/11/15 11:14:16	8.1	154.32E	46.75N	kisza12*4.0 + kiszb12*0.5 + kisza13*2.0 + kiszb13*1.5
Tonga *	2006/05/03 15:26:39	8.1	174.164W	20.13N	ntszb29 * 6.6
Rat Island	2003/11/17 06:43:07	7.8	178.74E	51.13N	acszb11 * 2.81
Andreanof	1996/06/10 04:03:35	7.8	176.847E	51.478N	acsza15*2.4 + acszb16*0.8
Kuril	1994/10/04 13:22:58	8.1	147.328E	43.706N	kisza20*9.0
Alaska	1964/03/28 03:35:14	9.0	147.73W	61.04N	Tang *et al* (2006)
Unimak	1946/04/01 12:28:56	8.5	163.5E	52.75N	acszb22 * 1.6 + acszb23 * 8.4 + acszb24 * 17.8

Table 4. Historical tsunami events modeled. Events for which tide gauge records are available at Craig are marked with *.

DRAFT

3.2 Model stability and reliability

Model stability testing verifies that the forecast model will remain numerically stable and produce reasonable results under a wide range of possible source scenarios. To test stability during large events, 50 M_w 8.3 seismic scenarios, and 50 M_w 9.3 seismic scenarios were created along all of the Pacific Ocean source zones in SIFT's propagation database (Gica *et al* 2008).

For the M_w 9.3 scenarios, twenty unit sources were assigned a uniform slip of 25.0 m. For the M_w 8.3 scenarios, four unit sources were assigned a uniform slip of 3.95 m. Table 5 contains the source combinations used and the resulting maximum wave heights at the Craig tide gauge site.

Sources closest to the Craig tide gauge produce the largest wave for both the M_w 8.3 (Figure 7) and M_w 9.3 (Figure 8) scenarios. Scenario acsz5, which places the seismic epicenter within the A grid of the forecast model, produces the largest wave for both seismic magnitudes tested. Far-field scenarios that produce above-average waves include ngsz1 and ngsz2, located on the north side of New Guinea, and kisz1yz, located at the north end of the Kamchatka subduction zone.

In addition to testing the model with large events, a no-wave test ensures that the model is internally stable, and does not generate a signal in the absence of substantial input waves. Testing was performed with a single distant source

with slip 5.0×10^{-5} m, producing waves less than 1.5×10^{-5} cm at A grid. Initial testing found that two points in the C grid, and one in the A grid, did produce waves over 1 cm under these conditions, but small-scale smoothing (modifying less than ten coastal grid points) removed these minor instabilities.

Scenario	M_w 8.3 scenarios		M_w 9.3 scenarios	
	Sources	Max. amp. (m)	Sources	Max. amp. (m)
acsz1	3.95 * acsz{ab}5-6	0.069	**25.0 * acsz{ab}1-10**	0.58
acsz2	3.95 * acsz{ab}15-16	0.085	25.0 * acsz{ab}11-20	0.64
acsz3	3.95 * acsz{ab}25-26	0.12	25.0 * acsz{ab}21-30	1
acsz4	**3.95 * acsz{ab}35-36**	0.29	25.0 * acsz{ab}31-40	3.3
acsz5	3.95 * acsz{ab}45-46	0.38	25.0 * acsz{ab}41-50	5.7
acsz6	3.95 * acsz{ab}55-56	0.21	25.0 * acsz{ab}51-60	2.2
acsz7	3.95 * acsz{ab}64-65	0.17	25.0 * acsz{ab}56-65	1.6
cssz1	3.95 * cssz{ab}5-6	0.035	25.0 * cssz{ab}1-10	0.23
cssz2	3.95 * cssz{ab}15-16	0.024	25.0 * cssz{ab}11-20	0.19
cssz2yz	3.95 * cssz{yz}19-20	0.014	25.0 * cssz{yz}15-24	0.25
cssz3	3.95 * cssz{ab}25-26	0.032	25.0 * cssz{ab}21-30	0.26
cssz4	3.95 * cssz{ab}35-36	0.033	**25.0 * cssz{ab}31-40**	0.2
cssz5	3.95 * cssz{ab}45-46	0.028	25.0 * cssz{ab}41-50	0.24
cssz6	3.95 * cssz{ab}55-56	0.027	25.0 * cssz{ab}51-60	0.23
cssz6yz	3.95 * cssz{yz}57-58	0.028	25.0 * cssz{yz}53-62	0.57
cssz7	3.95 * cssz{ab}65-66	0.037	25.0 * cssz{ab}61-70	0.3
cssz8	3.95 * cssz{ab}75-76	0.045	25.0 * cssz{ab}71-80	0.3
cssz9	3.95 * cssz{ab}85-86	0.04	25.0 * cssz{ab}81-90	0.33
cssz10	3.95 * cssz{ab}95-96	0.033	25.0 * cssz{ab}91-100	0.3
cssz10yz	3.95 * cssz{yz}100-101	0.048	25.0 * cssz{yz}96-105	0.62
cssz11	3.95 * cssz{ab}105-106	0.058	25.0 * cssz{ab}101-110	0.57
cssz11yz	3.95 * cssz{yz}110-111	0.071	25.0 * cssz{yz}106-115	0.71
cssz12	3.95 * cssz{ab}114-115	0.035	25.0 * cssz{ab}106-115	0.6
epsz1	3.95 * epsz{ab}5-6	0.072	25.0 * epsz{ab}1-10	0.93
epsz2	3.95 * epsz{ab}15-16	0.054	25.0 * epsz{ab}9-18	0.57
kisz1	3.95 * kisz{ab}5-6	0.051	25.0 * kisz{ab}1-10	0.77
kisz1yz	3.95 * kisz{yz}5-6	0.085	25.0 * kisz{yz}1-10	1.6
kisz2	3.95 * kisz{ab}15-16	0.053	25.0 * kisz{ab}11-20	0.43
kisz2yz	3.95 * kisz{yz}15-16	0.047	25.0 * kisz{yz}11-20	0.93
kisz3	3.95 * kisz{ab}25-26	0.061	25.0 * kisz{ab}21-30	0.7
kisz3yz	3.95 * kisz{yz}25-26	0.058	25.0 * kisz{yz}21-30	0.85
kisz4	**3.95 * kisz{ab}35-36**	0.048	25.0 * kisz{ab}31-40	0.51
kisz5	3.95 * kisz{ab}45-46	0.033	25.0 * kisz{ab}41-50	0.66
kisz6	3.95 * kisz{ab}55-56	0.061	25.0 * kisz{ab}51-60	0.51
kisz7	3.95 * kisz{ab}65-66	0.08	25.0 * kisz{ab}61-70	0.85
kisz8	3.95 * kisz{ab}74-75	0.076	25.0 * kisz{ab}66-75	0.93
mosz1	3.95 * mosz{ab}5-6	0.073	25.0 * mosz{ab}1-10	0.95
mosz2	3.95 * mosz{ab}15-16	0.051	25.0 * mosz{ab}8-17	0.48
ngsz1	3.95 * ngsz{ab}5-6	0.075	25.0 * ngsz{ab}1-10	1.1
ngsz2	3.95 * ngsz{ab}14-15	0.044	**25.0 * ngsz{ab}6-15**	1.2
ntsz1	3.95 * ntsz{ab}5-6	0.041	25.0 * ntsz{ab}1-10	0.44
ntsz2	3.95 * ntsz{ab}15-16	0.064	25.0 * ntsz{ab}11-20	0.42
ntsz3	**3.95 * ntsz{ab}25-26**	0.052	25.0 * ntsz{ab}21-30	0.64

DRAFT

ntsz4	3.95 * ntsz{ab}35-36	0.052	25.0 * ntsz{ab}30-39	0.69
nvsz1	3.95 * nvsz{ab}5-6	0.049	25.0 * nvsz{ab}1-10	0.53
nvsz2	3.95 * nvsz{ab}15-16	0.056	25.0 * nvsz{ab}11-20	0.35
nvsz3	3.95 * nvsz{ab}25-26	0.07	25.0 * nvsz{ab}21-30	0.58
nvsz4	3.95 * nvsz{ab}35-36	0.079	25.0 * nvsz{ab}28-37	0.85
rnsz1	3.95 * rnsz{ab}5-6	0.041	25.0 * rnsz{ab}1-10	0.26
rnsz2	3.95 * rnsz{ab}15-16	0.039	25.0 * rnsz{ab}11-20	0.37

Table 5. Source combinations and maximum forecast wave heights (at Craig tide gauge) for stability and reliability test scenarios. See Gica *et al*. 2008 for details of source locations. Sources highlighted in bold were used for the grid sensitivity comparison described in section 2.2.3.

4 Summary and Conclusions

This report describes the development of a real-time tsunami forecast model for Craig, Alaska. The forecast model grids were designed by comparing the results from multiple candidate grids to a reference model, for a variety of source scenarios. This algorithm for developing an optimal grid configuration may, with further refinement, be possible to automate, speeding inundation forecast model development.

The resulting forecast model is capable of producing real-time wave height forecasts that compare well with a higher-resolution reference model used for validation.

5 Acknowledgments

Yong Wei, Burak Uslu, Elena Tolkova, and Nazila Merati provided helpful comments and assistance. Paul Whitmore and Guy Urban provided tide gauge records and details about the WCATWC tide gauge installation at Craig.

PMEL publication number: ########

6 References

Amante, C. and B. W. Eakins. 2008. *ETOPO1 1 Arc-Minute Global Relief Model: Procedures, Data Sources and Analysis*, National Geophysical Data Center, NESDIS, NOAA, U.S. Department of Commerce, Boulder, CO.

Associated Press. 2002. Retired I-90 floating-bridge pontoons still working. August 19.

Burwell, D. 2008. Development of the Stand By Inundation Model for Sitka, Alaska. NOAA Tech. Memo., forthcoming.

Gica, E., M. Spillane, V.V. Titov, C.D. Chamberlin, and J.C. Newman. 2008. Development of the forecast propagation database for NOAA's Short-term Inundation Forecast for Tsunamis (SIFT). NOAA Tech. Memo. OAR PMEL-139, NTIS: PB2008-109391, 89 pp.

Lander, James F. 1996. *Tsunamis Affecting Alaska 1737-1996*, KGRD No. 31, National Oceanic and Atmospheric Administration, National Geophysical Data Center, Boulder, Colorado, USA, September, 155 p.

Smith, W. H. F., and D. T. Sandwell, 1997. Global seafloor topography from satellite altimetry and ship depth soundings, *Science*, v. 277, p. 1957-1962, 26 Sept.

DRAFT

Synolakis, C.E., E.N. Bernard, V.V. Titov, U. Kânoğlu, and F.I. González. 2007. Standards, criteria, and procedures for NOAA evaluation of tsunami numerical models. NOAA Tech. Memo. OAR PMEL-135, NOAA/Pacific Marine Environmental Laboratory, Seattle, WA, 55 pp.

Tang, L., V.V. Titov, C.D. Chamberlin. 2009. Development, testing, and applications of site-specific tsunami inundation models for real-time forecasting. *J. Geophys. Res.*, doi:10.1029/2009JC005476, in press.

Taylor, L.A, B.W. Eakins, E. Lim, R.R. Warnken, K.S. Carignan, P.R. Medley. 2008. Digital elevation models of Craig, Alaska: procedures, data sources, and analysis. National Geophysical Data Center, NOAA, U.S. Department of Commerce, Boulder, CO.

7 Appendix A

SIM MOST parameter file (most3_facts_nc.in):

```
0.0001 Minimum amp. of input offshore wave (m)
2.0    Minimum depth of offshore (m)
0.1    Dry land depth of inundation (m)
0.0015 Friction coefficient (n**2)
1      Let A-Grid and B-Grid run up
300.0  Max eta before blow-up (m)
1.0    Time step (sec)
21600  Total number of time steps in run (6 hours)
6      Time steps between A-Grid computations
3      Time steps between B-Grid computations
30     Time steps between output steps
0      Time steps before saving first output step
1      Save output every n-th grid point
gridA
gridB
gridC
./
./
1 1 1 1      NetCDF output for A, B, C, SIFT
6            Timeseries locations:
3 130 81     Craig tide gauge (226.857871, 55.488535)
3 118 94     Craig NW side (226.847871, 55.477701)
2 109 145    Bucarelli Bay Ent. (226.461620, 55.239120)
2 144 108    S of St. Ignace I (226.578287, 55.362454)
1 80 84      1000m contour S (225.649954, 54.883287)
1 42 49      1000m contour N (224.383287, 56.049954)
```

DRAFT

RIM MOST parameter file (most3_facts_nc.in):

```
0.0001 Minimum amp. of input offshore wave (m)
2.0    Minimum depth of offshore (m)
0.1    Dry land depth of inundation (m)
0.002  Friction coefficient (n**2)
1      Let A-Grid and B-Grid run up
300.0  Max eta before blow-up (m)
0.300000     Time step (s)
48000  Total number of time steps in run (4.0 hours)
6      Time steps between A-grid computations
2      Time steps between B-grid computations
108    Time steps between output steps
0      Time steps before saving first output step
2      Save output every n-th grid point
gridA
gridB
gridC
./
./
1 1 1 1      NetCDF output for A, B, C, SIFT
6            Timeseries locations:
3 569 491    Craig tide gauge (226.857824, 55.488889)
3 533 544    Craig NW side (226.847824, 55.477847)
2 676 674    Bucarelli Bay Ent. (226.462870, 55.239537)
2 816 527    S of St. Ignace I (226.579537, 55.362037)
1 400 419    1000m contour S (225.663287, 54.876620)
1 208 241    1000m contour N (224.383287, 56.063287)
```

DRAFT

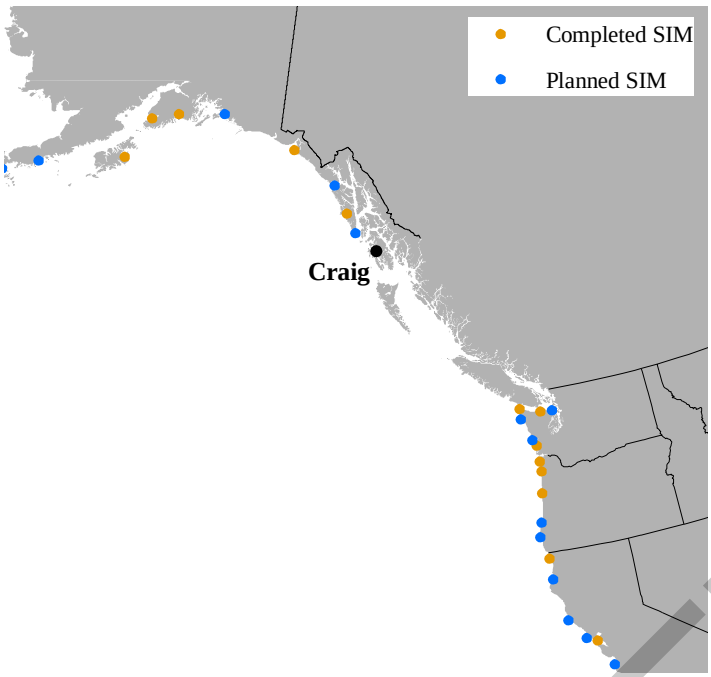

Figure 1. Location of Craig, Alaska, relative to other planned and completed forecast models.

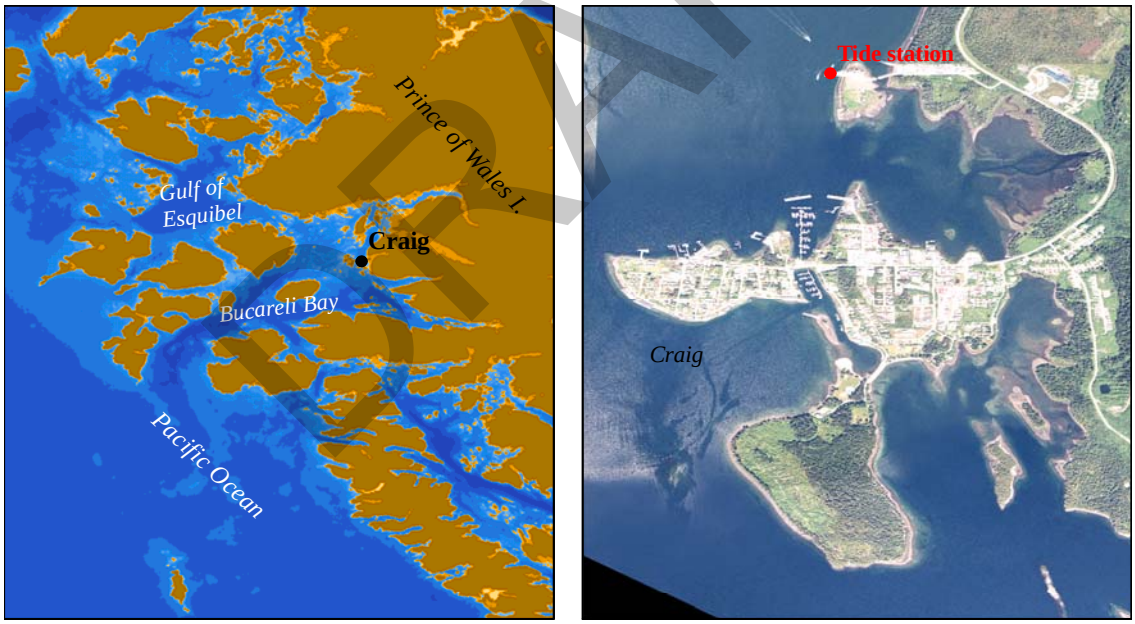

Figure 2. (a) Location of Craig, Alaska on the west side of Prince of Wales Island, partially protected from the open ocean by several offshore islands. (b) Aerial photograph of Craig, showing the town center and location of the tide station operated by the West Coast/Alaska Tsunami Warning Center.

DRAFT

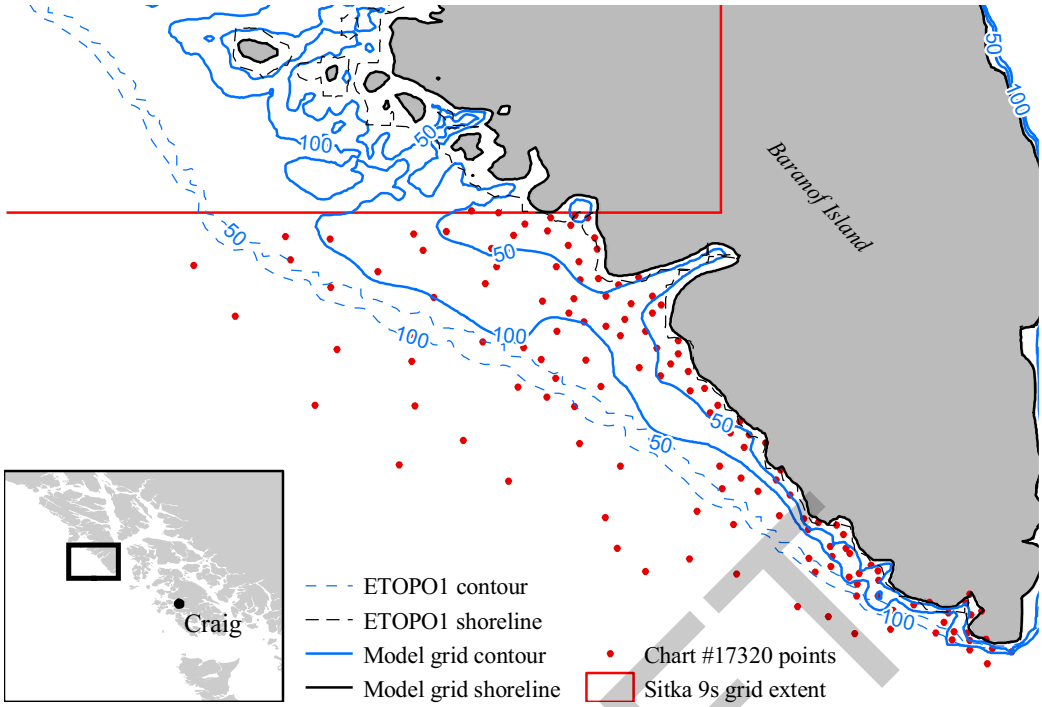

Figure 3. Comparison of bathymetry along southeastern Baranof Island. Original ETOPO1 bathymetry (dashed contours) is substantially improved in the model grid (solid contours) by the addition of existing medium-resolution bathymetry, and digitized points from NOS charts.

DRAFT

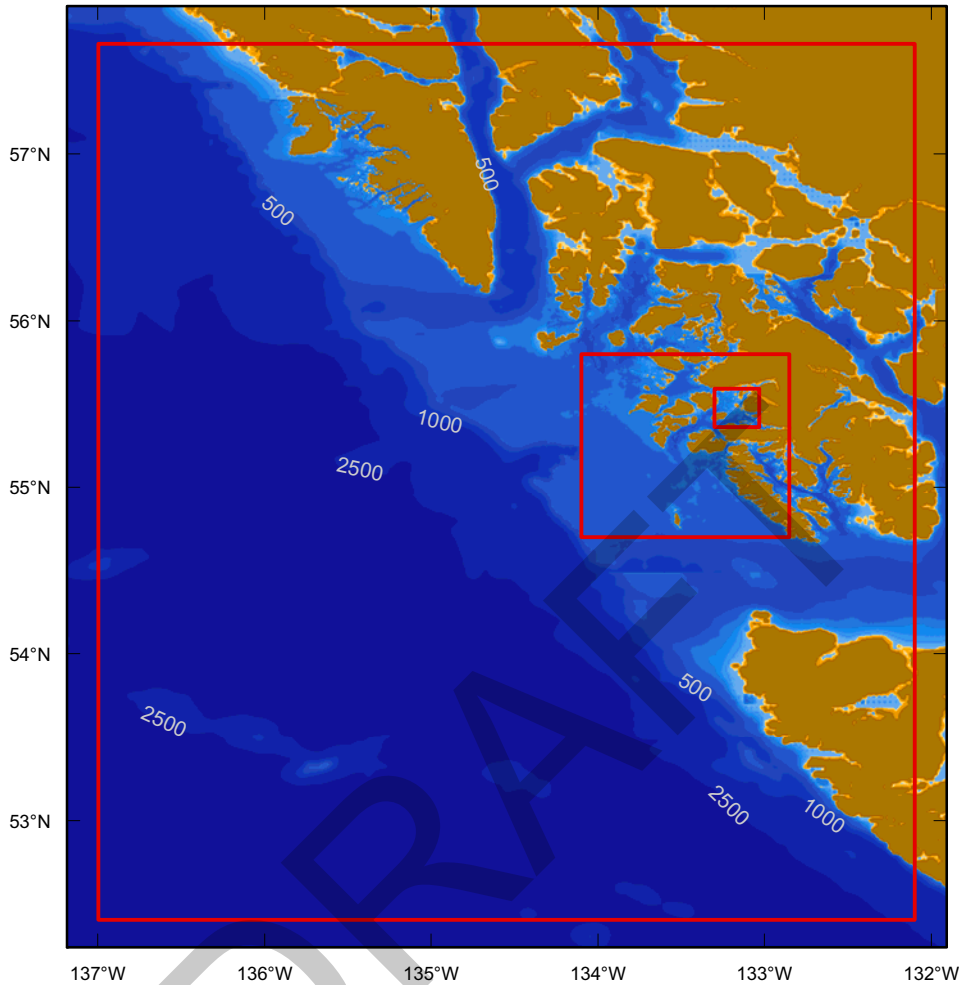

Figure 4. Reference inundation model (RIM) grid extents.

DRAFT

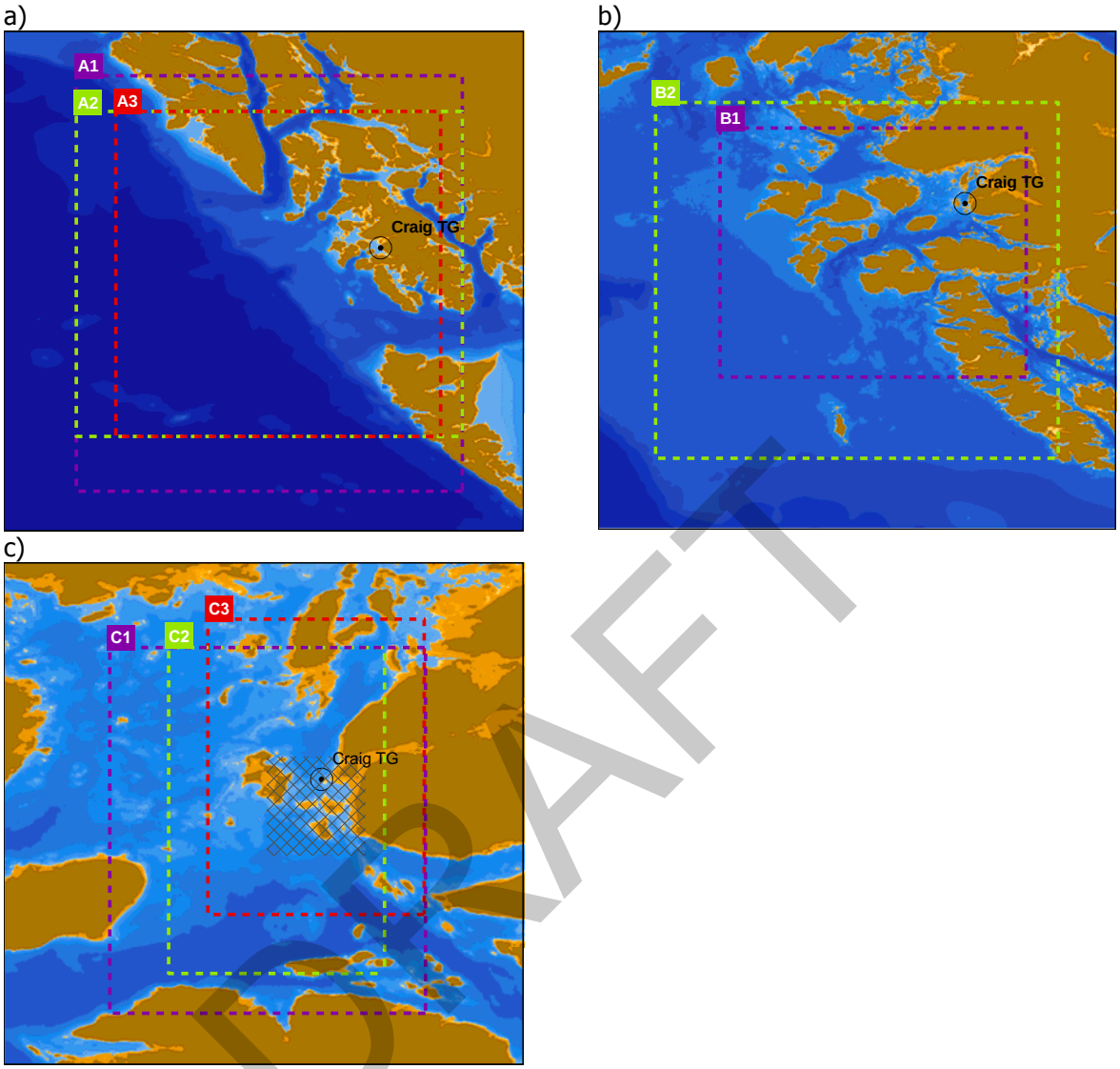

DRAFT

Figure 5. Extents of candidate forecast model (SIM) grids. Crosshatched area in (c) is the region where maximum wave comparisons with the reference model (RIM) are performed. See Table 1 for details of grid extents and resolutions.

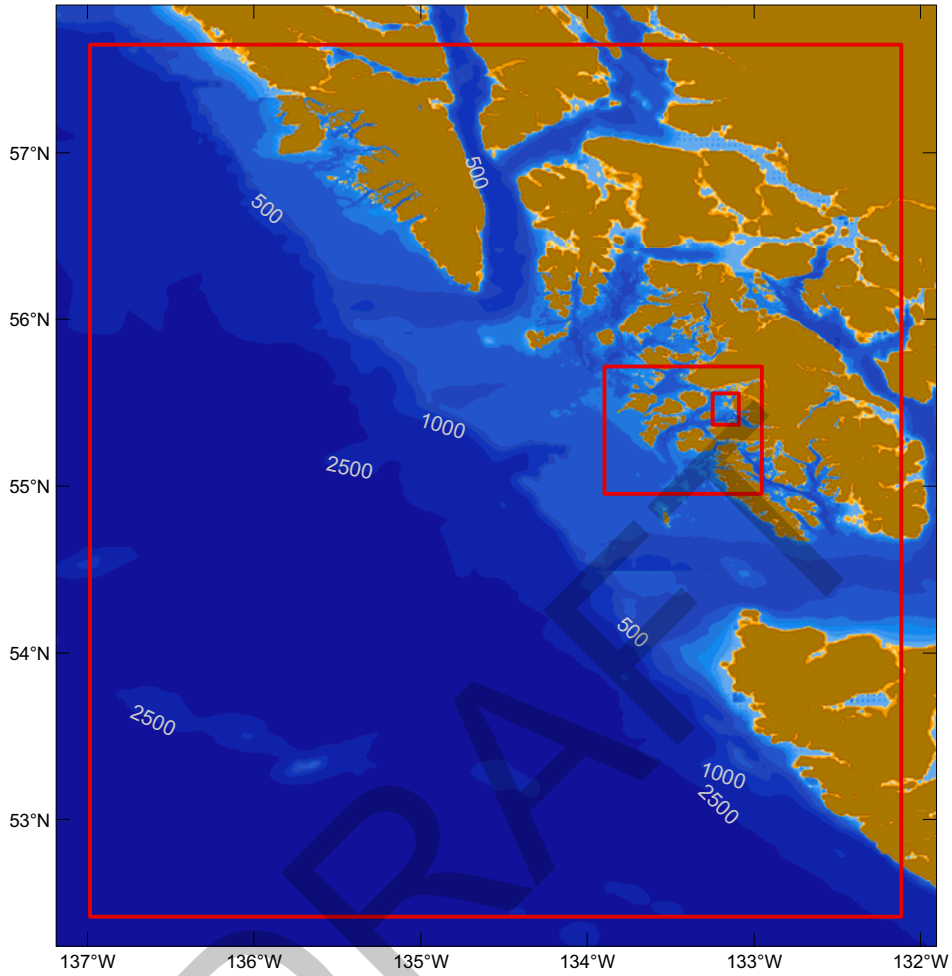

Figure 6. Forecast model (SIM) grid extents.

DRAFT

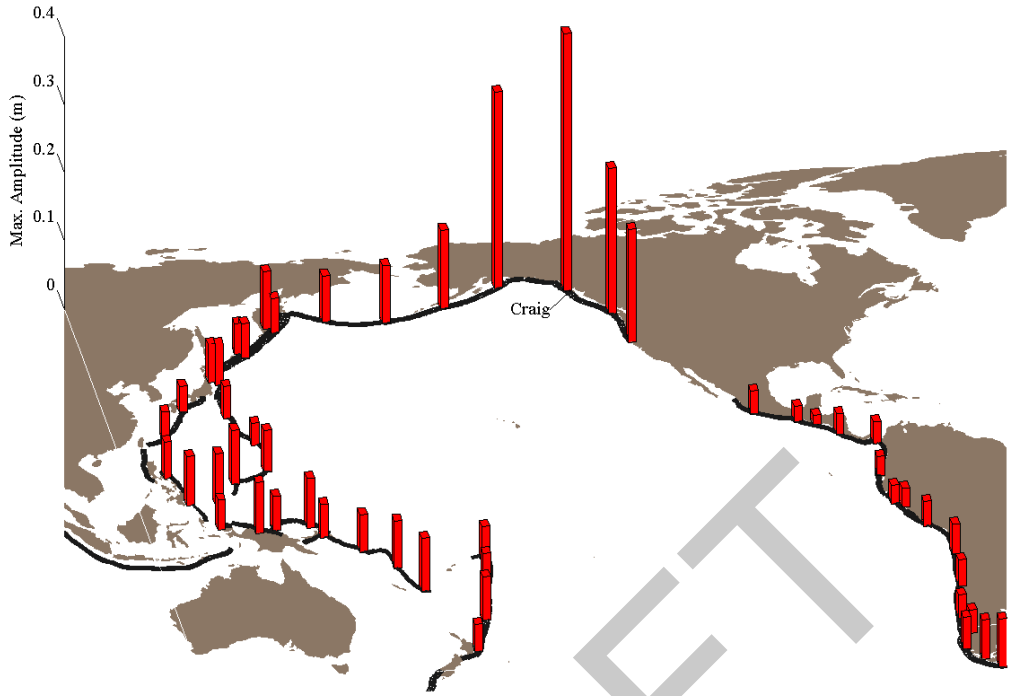

Figure 7. Maximum wave heights at Craig tide gauge for M_w 8.3 seismic scenarios.

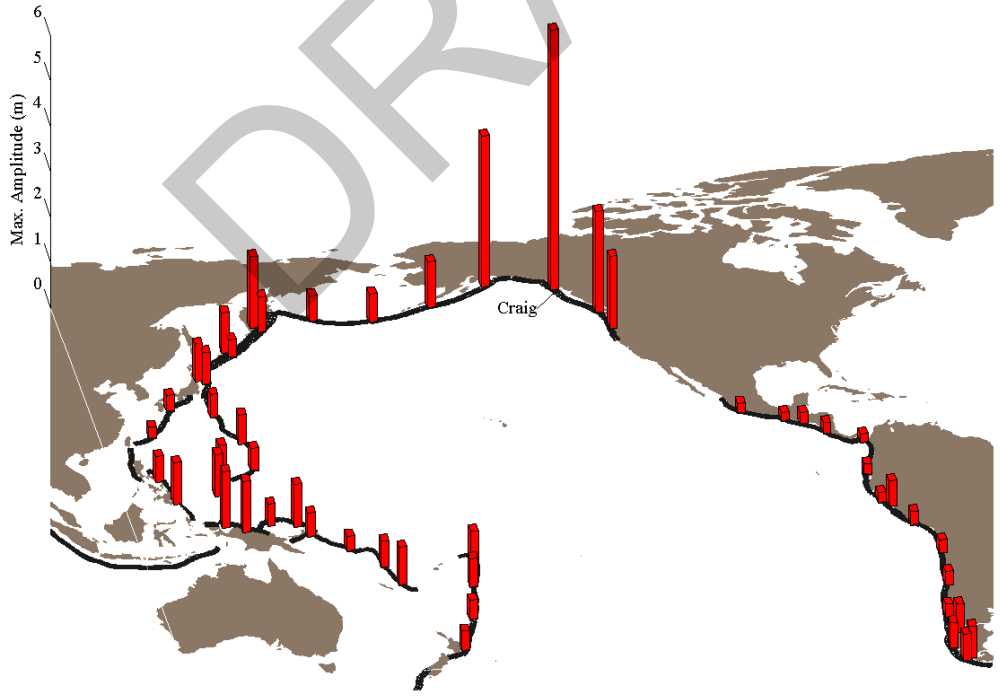

Figure 8. Maximum wave heights at Craig tide gauge for M_w 9.3 seismic scenarios.

DRAFT

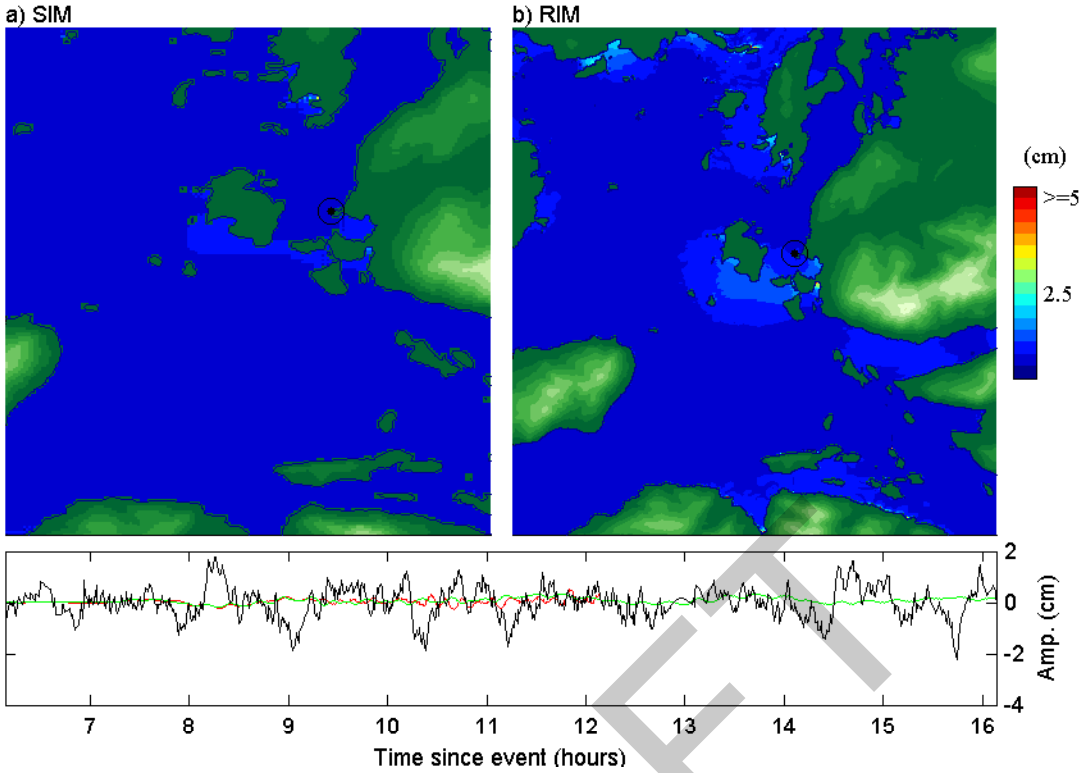

Figure 9. 15 January 2009 Kuril tsunami. (a) Forecast model (SIM) maximum amplitude plot. (b) Reference model (RIM) maximum amplitude plot. (c) Wave amplitude at tide gauge. Green: Forecast model (SIM); Red: Reference model (RIM); Black: tide gauge record.

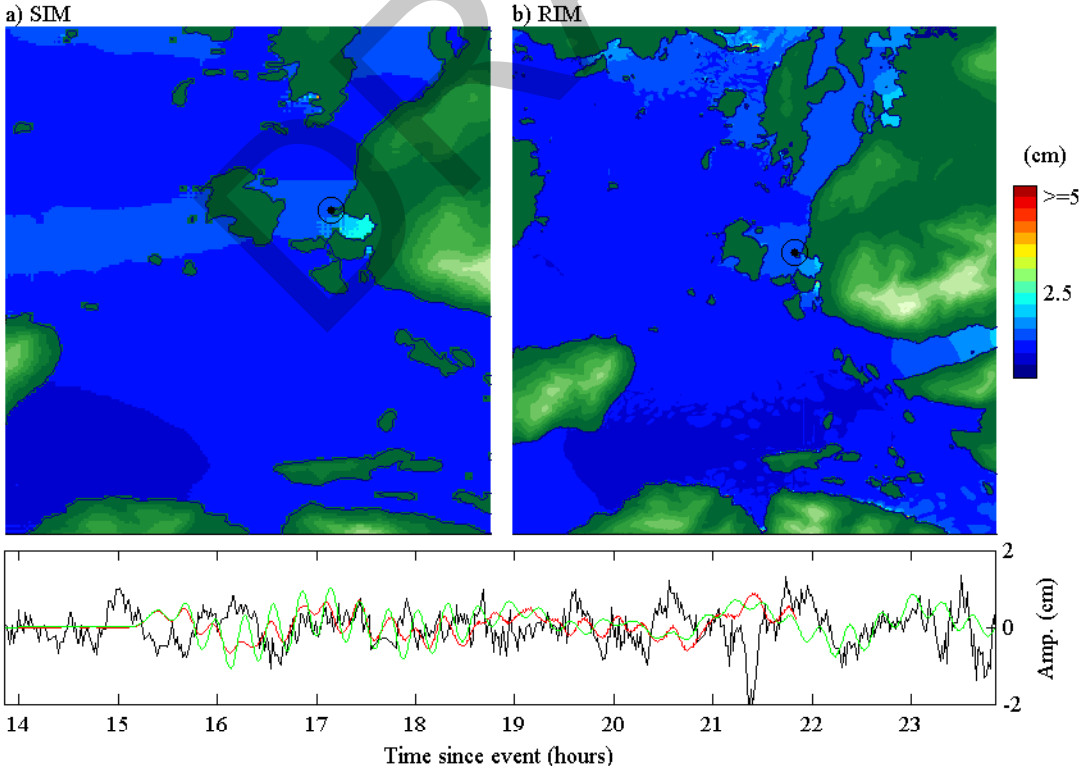

DRAFT

Figure 10. 15 August 2007 Peru tsunami. (a) Forecast model (SIM) maximum amplitude plot. (b) Reference model (RIM) maximum amplitude plot. (c) Wave amplitude at tide gauge. Green: Forecast model (SIM); Red: Reference model (RIM); Black: tide gauge record.

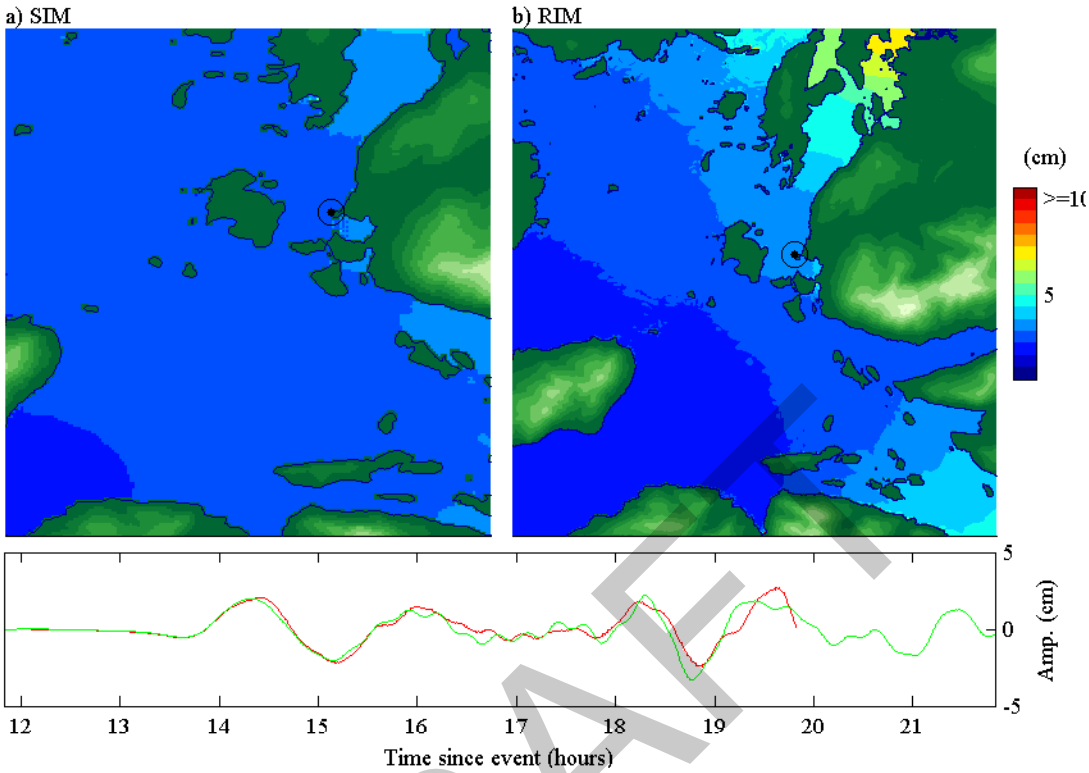

Figure 11. 1 April 2007 Solomon tsunami. (a) Forecast model (SIM) maximum amplitude plot. (b) Reference model (RIM) maximum amplitude plot. (c) Wave amplitude at tide gauge. Green: Forecast model (SIM); Red: Reference model (RIM).

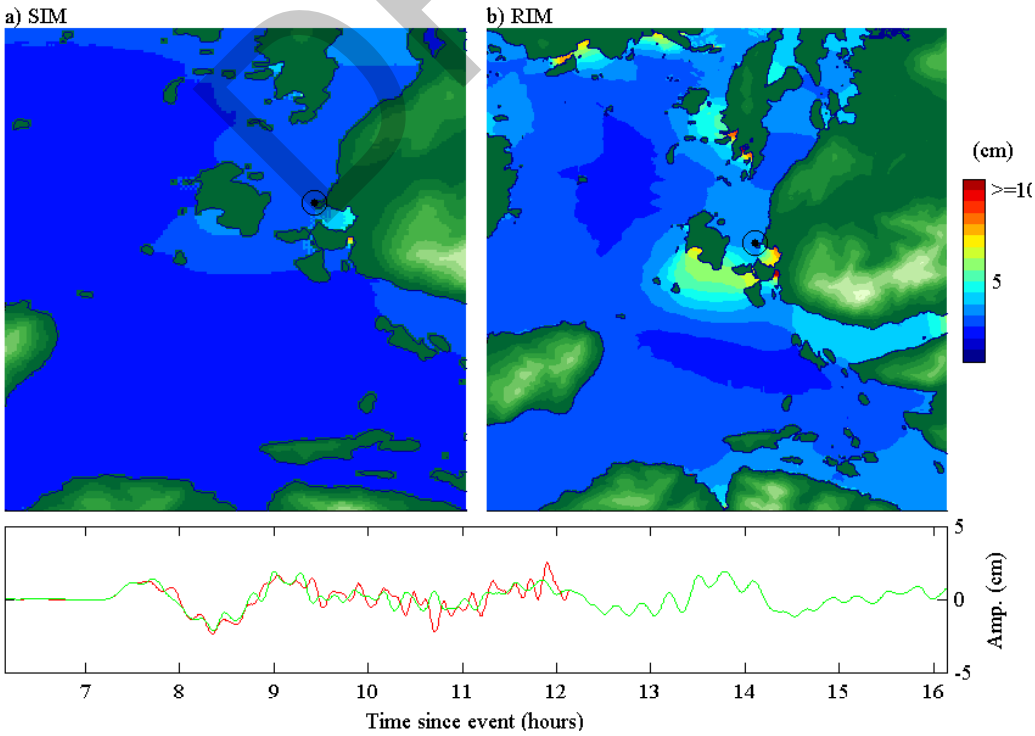

DRAFT

Figure 12. 15 November 2006 Kuril tsunami. (a) Forecast model (SIM) maximum amplitude plot. (b) Reference model (RIM) maximum amplitude plot. (c) Wave amplitude at tide gauge. Green: Forecast model (SIM); Red: Reference model (RIM).

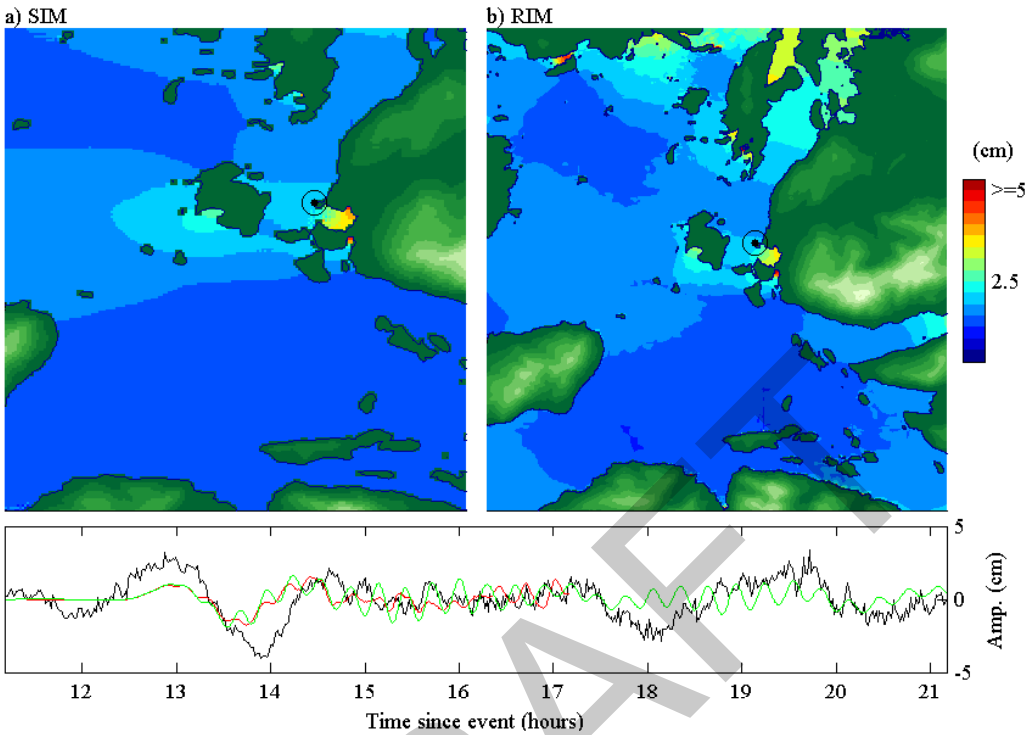

Figure 13. 3 May 2006 Tonga tsunami. (a) Forecast model (SIM) maximum amplitude plot. (b) Reference model (RIM) maximum amplitude plot. (c) Wave amplitude at tide gauge. Green: Forecast model (SIM); Red: Reference model (RIM).

DRAFT

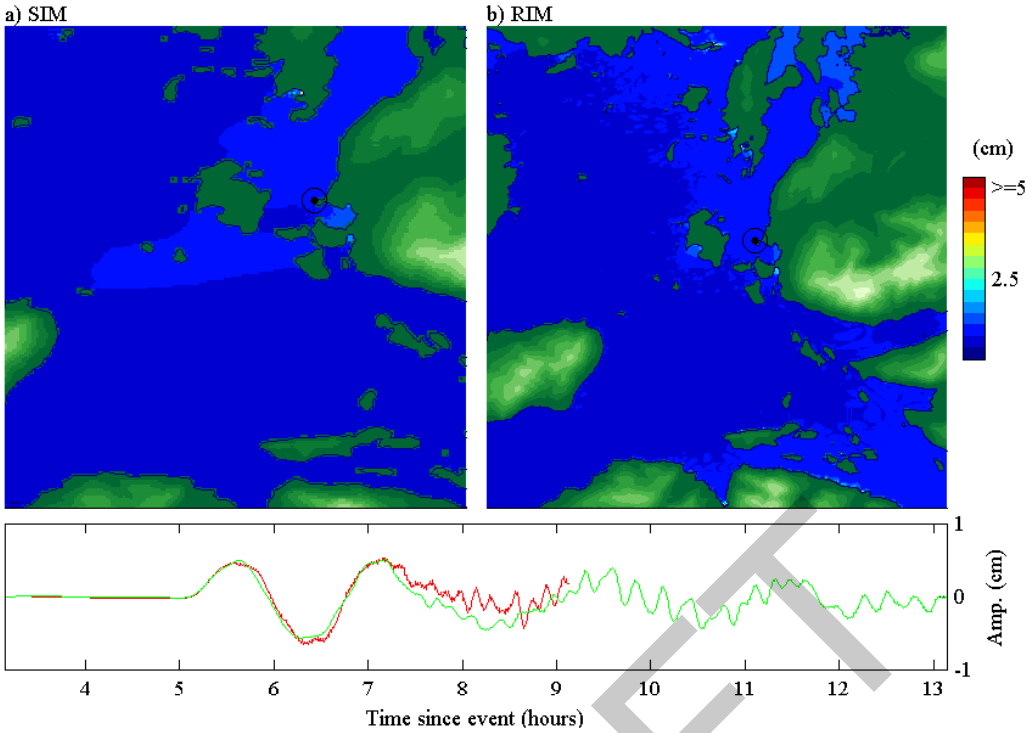

Figure 14. 17 November 2003 Rat Island tsunami. (a) Forecast model (SIM) maximum amplitude plot. (b) Reference model (RIM) maximum amplitude plot. (c) Wave amplitude at tide gauge. Green: Forecast model (SIM); Red: Reference model (RIM).

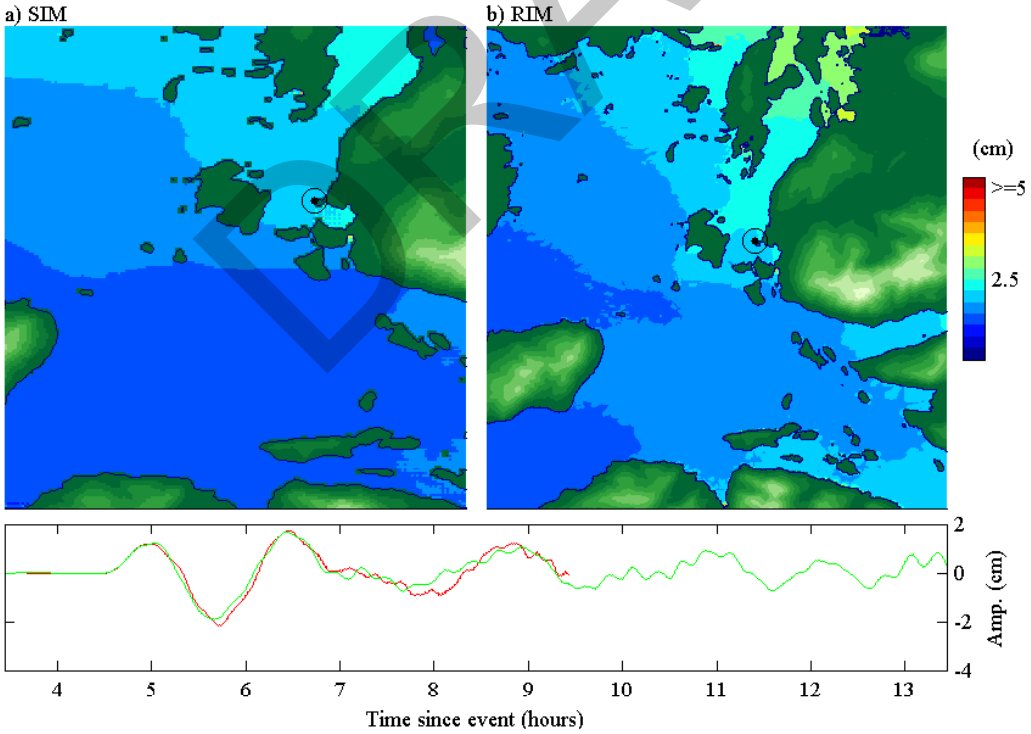

Figure 15. 10 June 1996 Andreanof tsunami. (a) Forecast model (SIM) maximum amplitude plot. (b) Reference model (RIM) maximum amplitude plot. (c) Wave amplitude at tide gauge. Green: Forecast model (SIM); Red: Reference model (RIM).

DRAFT

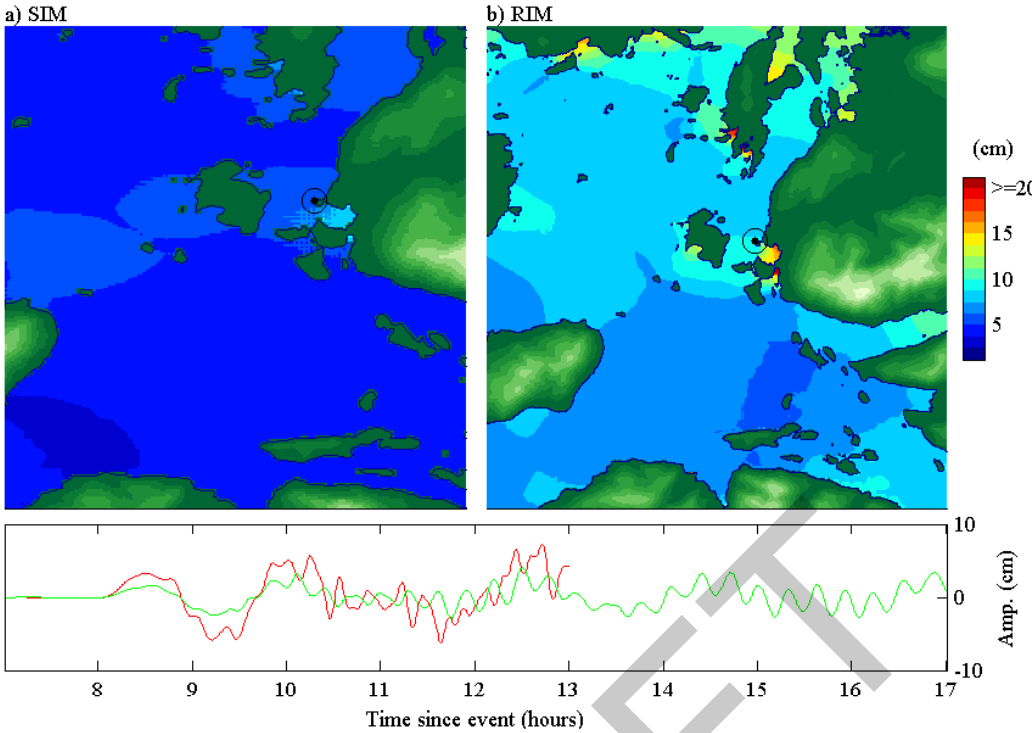

Figure 16. 4 October 1994 Kuril tsunami. (a) Forecast model (SIM) maximum amplitude plot. (b) Reference model (RIM) maximum amplitude plot. (c) Wave amplitude at tide gauge. Green: Forecast model (SIM); Red: Reference model (RIM).

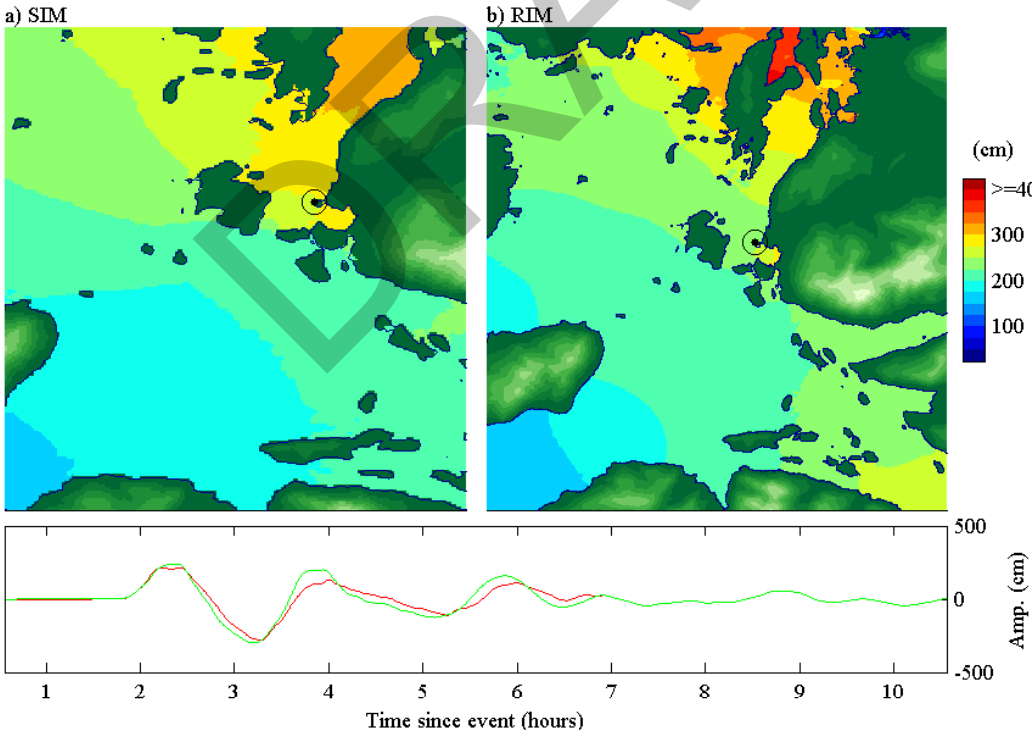

Figure 17. 28 March 1964 Alaska tsunami. (a) Forecast model (SIM) maximum amplitude plot. (b) Reference model (RIM) maximum amplitude plot. (c) Wave amplitude at tide gauge. Green: Forecast model (SIM); Red: Reference model (RIM).

DRAFT

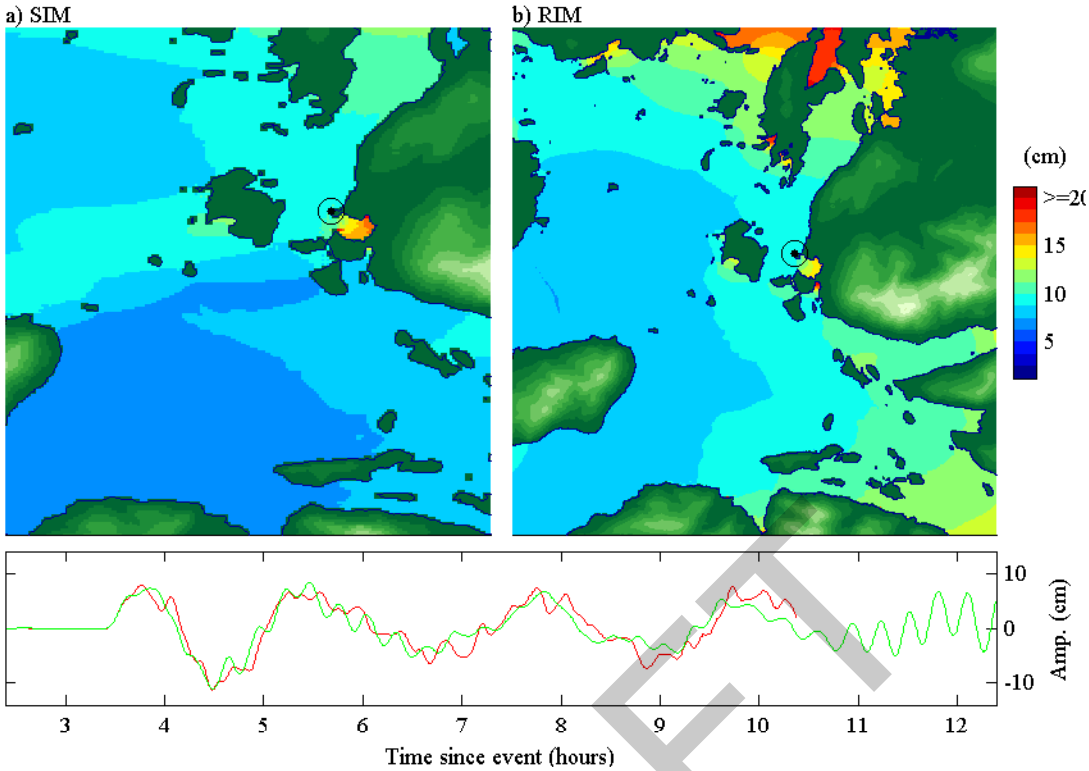

Figure 18. 1 April 1946 Unimak tsunami. (a) Forecast model (SIM) maximum amplitude plot. (b) Reference model (RIM) maximum amplitude plot. (c) Wave amplitude at tide gauge. Green: Forecast model (SIM); Red: Reference model (RIM).

DRAFT